Online-Journals.org

iJOE International Journal of Online and Biomedical Engineering

iJOE | eISSN: 2626-8493 | Vol. 20 No. 2 (2024) | OPEN ACCESS

https://doi.org/10.3991/ijoe.v20i02.46817

PAPER

Static, Dynamic, and High Cycle Fatigue Analysis of Crossed Spherical Gearing for Robotic Arm Ball Joint: A Finite Element Analysis Approach

José L. Serna-Landivar[1](✉), Madelaine Violeta Risco Sernaqué[2], Ana Beatriz Rivas Moreano[2], William C. Algoner[1], Daniela M. Anticona-Valderrama[3], Walter Enrique Zúñiga Porras[1], Carlos Oliva Guevara[1]

[1]Universidad Tecnológica del Perú, Lima, Perú

[2]Universidad Autónoma del Perú, Lima, Perú

[3]Universidad Privada del Norte, Lima, Perú

u18101283@utp.edu.pe

ABSTRACT

Crossed spherical gearing is used in the joints of robotic arm prostheses and allows mobility in 3 degrees of freedom. This paper aims to evaluate the design of a cross-spherical gear with three different materials, PEEK, AISI 304L, and Ti-6Al-4V, for a robotic arm prosthesis by finite element analysis. ANSYS mechanical software (version 2021 R1) was used to perform the static analysis and evaluate the deformations and stresses, modal analysis of natural frequencies and vibration modes, and high cycle fatigue analysis to determine fatigue resistance. The results obtained in the static analysis show that the maximum stresses are in the same zones for the three materials and have similar values. However, the Ti-6Al-4V and ASI 304L materials have a higher safety factor than PEEK, with a value of 5.17. In conclusion, the crossed spherical gearing is numerically validated using the finite element analysis so that the prototype can be later manufactured at an experimental level, and the values obtained for the crossed spherical gearing of the robotic arm prosthesis can be verified.

KEYWORDS

crossed spherical gearing, static analysis, modal analysis, fatigue analysis, robotic arm prosthesis

1 INTRODUCTION

Amputation of the upper limb is one of the leading causes of disability and probably occurs at all levels of the limbs. This problem urgently needs to be addressed and solutions found to provide a better quality of life to the millions of people who face the same conditions [1].

There are several mechanical design proposals to solve the problem of spherical rotational motion of a ball-and-socket joint. Spherical motion often occurs in

Serna-Landivar, J.L., Risco Sernaqué, M.V., Rivas Moreano, A.B., Algoner, W.C., Anticona-Valderrama, D.M., Zúñiga Porras, W.E., Guevara, C.O. (2024). Static, Dynamic, and High Cycle Fatigue Analysis of Crossed Spherical Gearing for Robotic Arm Ball Joint: A Finite Element Analysis Approach. *International Journal of Online and Biomedical Engineering (iJOE)*, 20(2), pp. 16–30. https://doi.org/10.3991/ijoe.v20i02.46817

Article submitted 2023-09-16. Revision uploaded 2023-11-08. Final acceptance 2023-11-25.

© 2024 by the authors of this article. Published under CC-BY.

mechanical systems such as robotic wrists, arms, orientation mechanisms, exoskeletons, etc. [2]–[5].

Spherical gears with multiple degrees of freedom are an emerging field that needs to be developed, which is why there are several designs, such as the one proposed by [6], where the spherical gears changed the discrete bevel teeth into circular arc teeth. The motion is transmitted through the meshing of convex circular arc teeth and concave circular arc teeth. Then, in [7], the authors designed spherical gears with a continuous convex-concave drum-shaped involute tooth profile. Other authors proposed a spherical gear with a different ring-shaped development tooth profile [8]. In another study by [9], the authors present a new type of spherical gear, which consists of the smooth development of the tooth surface of an annular development ring and the spherical development of the surface of a spherical bevel tooth with 3 degrees of freedom.

Similarly, the investigations of [10] and [11] addressed the Abenics design of a 3-degree freedom ball joint, comprising a crossed spherical gear and two monopolar gears; they used PEEK material for arm or wrist joint applications. However, they still need to address the static, fatigue, and dynamic analysis of the spherical gear in other materials used in the industry; therefore, more research must be evaluated using the finite element method.

Finite analysis helps predict and control the behavior of engineering materials and mechanical parts in various applications. Biomaterials are crucial in developing components that are durable and compatible with the human body. For example, PEEK (polyether ether ketone) polymers, AISI 304L stainless steel, and titanium alloys such as Ti6Al4V [12] and [13]. Research has shown that finite element modeling is an essential factor in the application of engineering materials because the behavior of unique materials can be accurately predicted before experimental validation, eliminating trial-and-error costs [14] and helping to predict mechanical and vibration properties of materials produced in the laboratory.

This paper aims to evaluate the mechanical strength of the three-degree-of-freedom ball and socket cross-spherical gear in terms of stress-strain behavior in a linear regime (static analysis), dynamic (modal analysis), and high-cycle fatigue behavior for static stress-strain behavior using a finite element analysis (ANSYS 2021 R2), Ti6Al4V titanium alloys, PEEK polymer, and AISI 304L stainless steel were used in the spherical crossover. In addition, the dynamic behavior was evaluated under the natural conditions to which the crossed spherical gear was subjected.

2 MATERIALS AND METHODS

2.1 3D finite element model

The simplified three-degree-of-freedom robotic prosthesis with a ball-joint consists of the prosthesis, the base of the spherical gear system, the cross-spherical gear, and the two monopolar gears (see Figure 1). The prosthesis serves to replace missing body parts or to make body parts function better.

Figure 2 shows a detailed 3D model of the ball joint with three degrees of freedom, with precision servomotors allowing the two monopolar gears to rotate, i.e., they are the drivers, so the spherical gear is the driven gear. This roll allows rotational rotation and is ideal for simulating a shoulder joint (ball and socket joint). However, it has its limits of rotation and turns, and the restriction is the base that supports the crossed spherical gear.

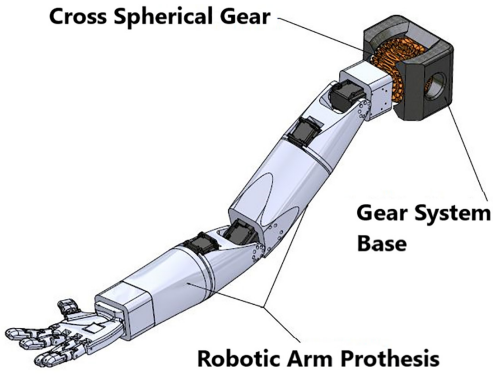

Fig. 1. 3D model of the three-degree-of-freedom ball-joint robotic arm prosthesis

The modeling of the ball joint was done in the CAD INVENTOR 2023 software. The modeling of the spherical gear took into account the research of the authors Abe et al. from their design of the ABENICS model [10], [11]; the crossed spherical gear is obtained from the principle of the straight tooth gearing, wich being the number of teeth equal to 30, the module is 3 mm, and the monopolar gears have 15 teeth with the same module (see Figure 3). It is then rotated through 360° in one plane, and then in another orthogonal plane, another cutting revolution is performed on the teeth generated in the first revolution. In addition, it consists of a coupling of the prosthesis to the spherical gear.

The numerical model of the crossed spherical gear is modeled in computer-aided software (CAD) called INVENTOR, then exported to ANSYS in step or igs format; these formats are ideal for the ANSYS simulation software to recognize the geometry and corresponding measurements. ANSYS is a powerful and complete software simulation that, using the finite elements method, allows us to solve mechanical problems and complex designs; its results are also reliable and fast.

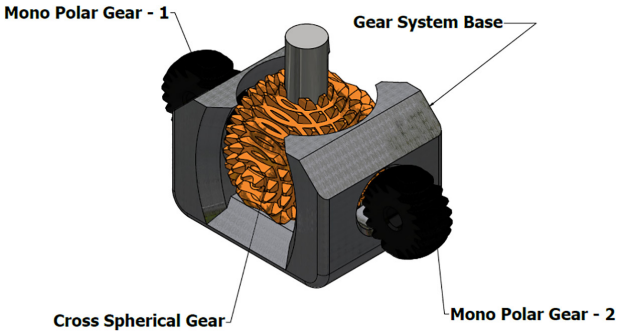

Fig. 2. 3D model of a three-degree-of-freedom ball-joint

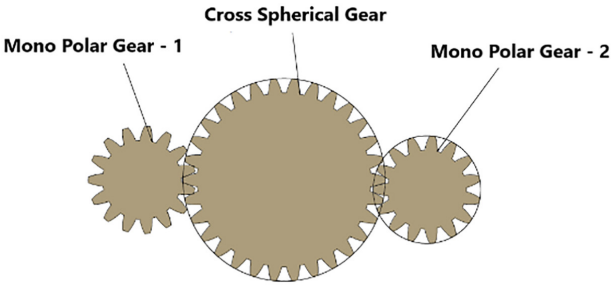

Fig. 3. Cross-section of the assembly of the spherical gear and the two monopolar gears

Table 1 defines the mechanical properties of PEEK material, Ti-6Al-4V titanium alloy, and AISI 304L stainless steel; these values were entered in the "engineer data" module. The entered values are modulus of elasticity, yield strength, Poisson's ratio, and density, which are sufficient variables to execute the simulation correctly.

For the fatigue strength and stress cycle number (S-N) curves of the three materials mentioned, the literature on fatigue strength of these materials was found; titanium alloy Ti-6Al-4V was found in references [15]–[18], PEEK material in [19] and stainless steel material AISI 304L [20].

In the meshing of the research object, a mesh convergence study was performed so that the entity is discretized, and the mesh is refined so that the value of the result does not have a significant deviation value. The result is 48404 nodes with 29325 elements. The average quality of the elements is 0.88, in the Ref. [21] a minimum mesh size of 0.7 is recommended. This shows that the quality of the elements is good, as shown in Figure 4, the modeling of the loop intersecting spherical gear, and in Figure 5, the tension loop convergence curve against the number of nodes.

Table 1. Mechanical properties of the material PEEK (Polyether ether ketone), Stainless steel (AISI 304L), and Titanium alloy Ti-6Al-4V

Material	Modulus of Elasticity (Gpa)	Yield Strength (Mpa)	Poisson Ratio	Density (Kg/m^3)	References
PEEK	3.45	95	0.4	1300	[22]–[24]
AISI 304 L	190	210	0.29	8000	[25]–[29]
Ti-6Al-4 V	114	880	0.31	4500	[14], [30]–[34]

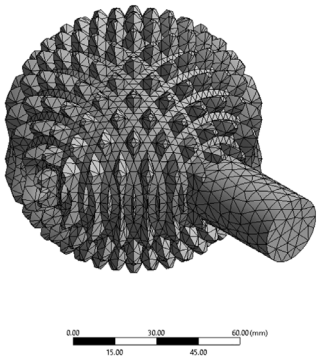

Fig. 4. Meshing of the cross-spherical gear

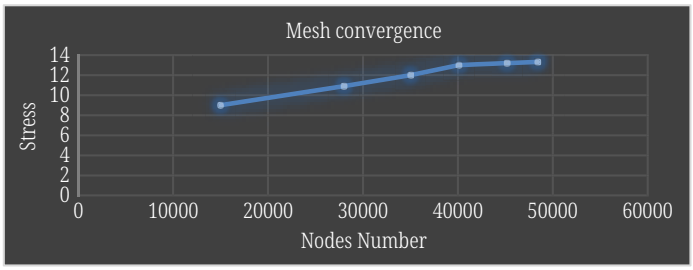

Fig. 5. Mesh convergence of finite element analysis

The boundary conditions used in the finite element analysis of the ANSYS Workbench platform are necessary because they determine the degrees of freedom of the object under study and the loads applied to it (see Figure 6).

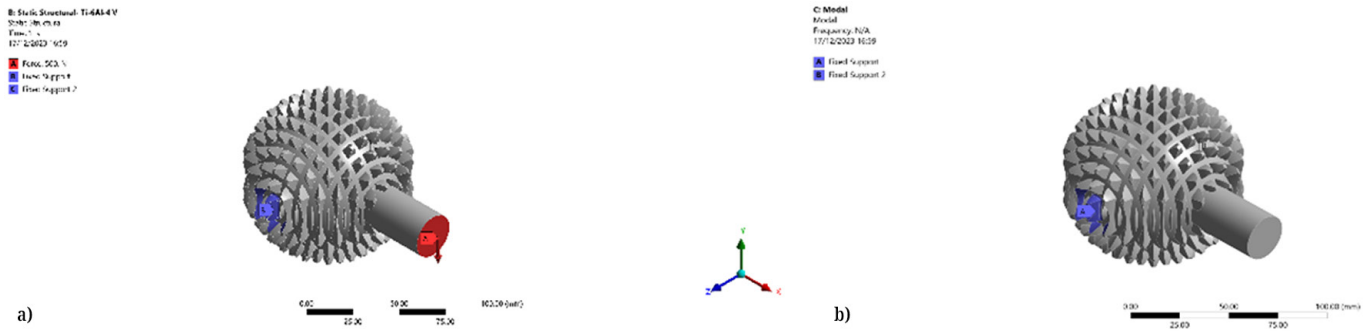

Fig. 6. Boundary conditions. a) static analysis and fatigue analysis b) modal analysis

2.2 Static analysis

On the other hand, with the static simulation carried out with ANSYS, the stresses, deformations, and safety factors will be found. This analysis is in the elastic range, i.e., linear. The mathematical equation that allows us to solve this problem is Eq. 1. [35], [36]:

$$F = Ku \tag{1}$$

Where:

[*F*]*: Matrix Force*
[*K*]*: Matrix stiffness*
[*U*]*: Vector displacement*

2.3 Modal analysis

It is essential to mention that it is vital to know the behavior of each engineering structure; with modal analysis, the dynamic behavior, such as natural frequencies and modes of vibration, can be determined under the condition that friction (damping) and external forces are neglected [37]–[39]. In the simulation, we will use ten vibration modes to capture the crucial frequencies and modes of vibration of the object of the research study.

Then, Eq. 2 is the linearized differential equation governing the dynamic behavior of the crossed spherical gear [40]–[45].

$$F(t) = [M\ddot{u}] + [C\dot{u}] + [Ku] \tag{2}$$

Where $F(t)$ is the time-varying force, $[M]$ the mass matrix, $[C]$ the damping matrix, $[K]$ the stiffness matrix, and u the acceleration, velocity, and nodal displacement vectors, respectively [46]–[48].

Simplifying Eq. 2, to find the natural frequencies of the object of study, reducing and considering that the damping value equals zero, we obtain the following equation 3, [45], [49]:

$$F(t) = ([M]\omega_i^2 + +[K])\{u\} \tag{3}$$

Where ω is the natural frequency, and u is the displacement vector, $F(t)$ is the time-varying force, $[M]$ the mass matrix y $[K]$ the stiffness matrix.

2.4 Fatigue analysis

Regarding fatigue analysis, the stress-life method was considered to evaluate the cross-spherical gear based on stress levels only; the object is subjected to repeated forces or loads of varying magnitude. This stress-life method is prevalent for applications in the design area and adequately represents high-cycling applications.

The S-N curve is a material fatigue curve that indicates the relationship between stresses and the number of cycles. Usually, the graph of the curve can be divided into two parts: one is the finite life region, and the other is the infinite life region. The infinite life region means that the stress level of the components is less than or equal to the fatigue limit, while the finite life region means that the stresses are higher than the fatigue stress limit of the material [21], [50], [51].

Equation 4 gives the steel's fatigue strength or yield strength S'_e, which can be approximated from the tensile strength data S_{ut}.

$$S'_e = 0.50\, S_{ut} \tag{4}$$

This property of the fatigue strength limit is fulfilled when the base material has an ultimate tensile strength [52].

The actual fatigue limit of a part may differ significantly from the one obtained from the S-N curve. This is because each S-N curve is obtained by experimentally testing in a laboratory a specific sample with a particular geometry with a unique surface finish, often very different from that of the part under conditions of load, temperature, etc. According to Marín [53], the new fatigue limit will be calculated from the previous theoretical limit obtained from the tests but affected by the different correction coefficients that consider the influence of the other factors according to the actual working conditions. Therefore, the Marin equation is expressed as follows:

$$S_e = K_a K_b K_c K_d K_e K_f S'_e \tag{5}$$

Where:

K_a: *Modification factor due to surface condition.*
K_b: *Modification factor by size.*
K_c: *Modification factor by load.*
K_d: *Modification factor due to temperature.*
K_e: *Reliability factor.*
K_f: *Modifying factor for miscellaneous effects.*
S_e: *Fatigue strength limit of laboratory sample specimen tests.*
S'_e: *Fatigue strength limit for rotating beam* (*steel tree*).

In the crossed spherical gear, the established factors of the Marin equation are considered, as it is essential to correct the fatigue strength limit to perform the finite element analysis in ANSYS Workbench.

3 RESULTS

3.1 Static analysis

The results obtained in the static analysis are the maximum stresses, as shown in Figure 7. The maximum stress of Ti-6Al-4V material is 13.32 MPa; the maximum stress of the PEEK material is 12.87 MPa; for AISI 304L material, the maximum stress is 13.37 MPa. In these three cases, the stress concentration is located at the gear tooth; thus, the safety factors for each material are 66.0, 7.38, and 15.7.

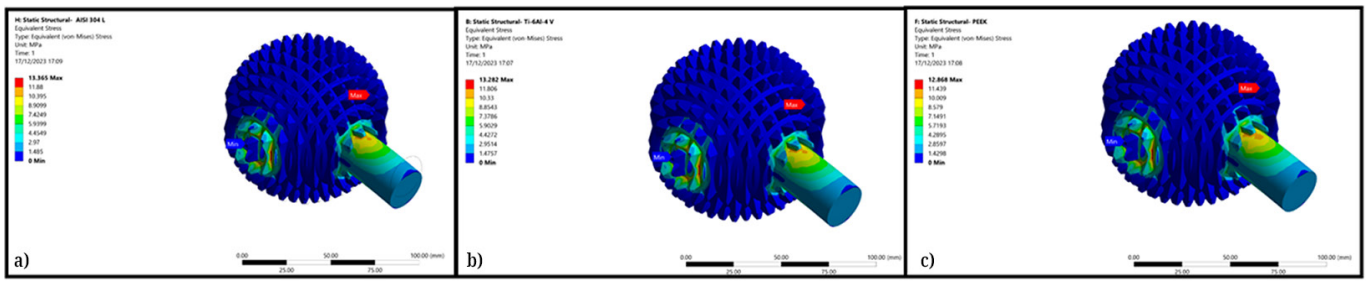

Fig. 7. Static analysis. a) Maximum stresses AISI 304L b) Maximum stresses Ti-6Al-4V c) Maximum stresses PEEK

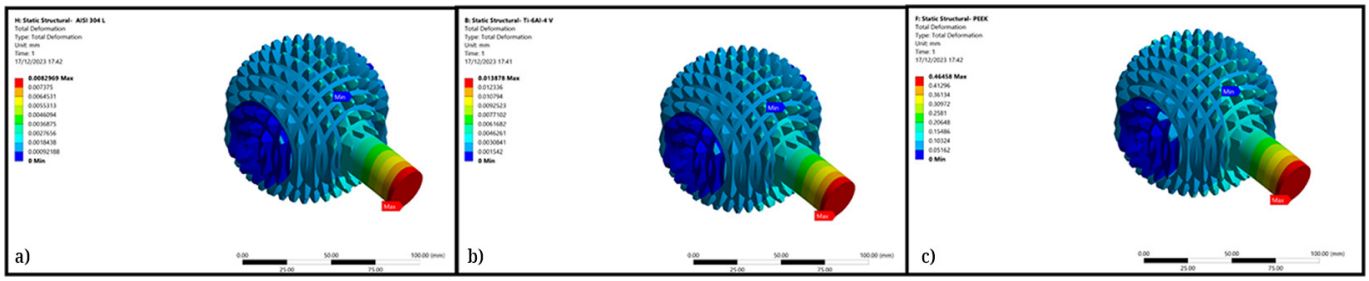

Fig. 8. Static analysis. a) maximum deflection AISI 304L b) maximum deflection Ti-6Al-4V c) maximum deflection PEEK

On the other hand, the deformations obtained in the static analysis are shown in Figure 8, and their values are the following: for the material AISI 304L, it has a value of 0.0083 mm; for the material PEEK, it has a value of 0.4646 mm, and finally, for the material Ti-6Al-4V, it has a value of 0.0079 mm; these values are within the permissible limits for this type of machine elements.

3.2 Modal analysis

The results of modal analysis using ANSYS shown in Table 2 and Figure 9 show that as the vibration mode order increases, the frequency also varies from 1002.1 Hz to 23664 Hz. Each material has its own natural frequency and vibration mode, so analyzing the behavior of each one, vibration mode 1 has a torsional behavior concerning the "Z" axis since it has mass participation of 98. 9 % of the total and vibration mode 3 has a bending behavior in the direction of the "Y" axis, as it has mass participation of 71 % of the total mass. These vibration modes are of interest as they behave similarly to the one the crossed spherical gear would be subjected to in natural conditions (See Figure 10).

Table 2. Natural frequencies and modes of vibration of the three materials studied

Mode	PEEK – Frequency [Hz]	AISI 304L – Frequency [Hz]	Ti-6Al-4V – Frequency [Hz]
1	1002.1	3090.6	3172.7
2	2287.2	6762.1	6996.1
3	2414.6	7376.1	7586.6
4	2556.7	7817.3	8037.4
5	3119.9	9303	9609.3
6	4068.7	11841	12278
7	4398.3	13319	13717
8	4560.1	13725	14150
9	5622	17469	17912
10	7652.1	22912	23664

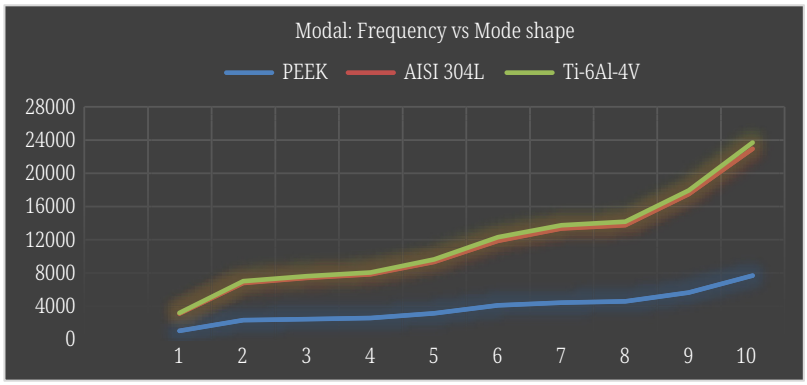

Fig. 9. Modal analysis: Frequency vs Mode shape vibration

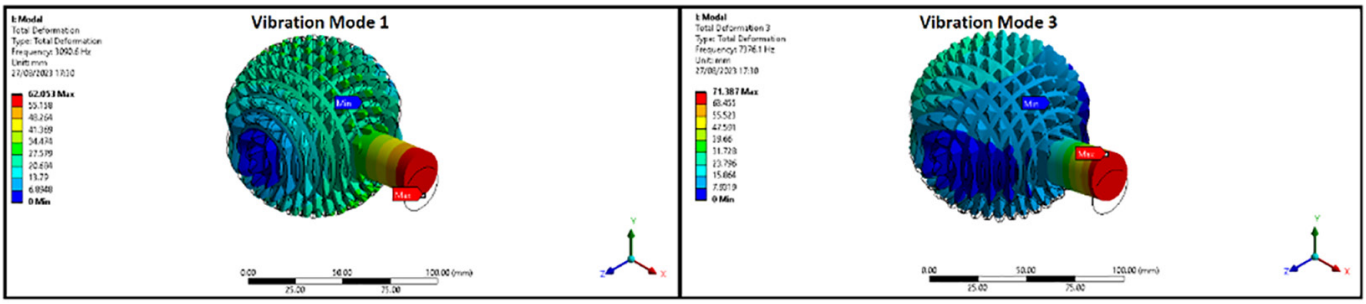

Fig. 10. Modal analysis: mode shape 1 and 2

3.3 Fatigue analysis

The stress-life method was considered in the high cycle fatigue analysis, as it is appropriate for this type of machine element. In Figure 11, the life of the crossed spherical gear is observed; it has a value of 10^6 in the whole object of study, so no stress is above the fatigue limit, which we can ensure that the element will not fail by fatigue.

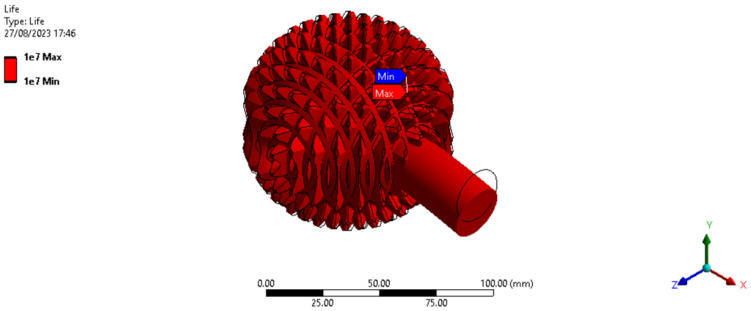

Fig. 11. Fatigue analysis: the life of the cross-spherical gearing of the three types of materials

The safety factor in the high cycle fatigue analysis is 5.17 in PEEK material (see Figure 12), considering that the fatigue strength limit is lower than the creep resistance in the static regime since the Marin factors were considered in the fatigue regime. However, stress concentrations exist in both fixed and fatigue analyses at the base of the teeth and tooth contact, as stated in the articles [54]–[60]. At the junction of the crossed spherical gear and the coupling, the teeth of the crossed spherical gear have an essential influence on the fatigue strength of a mechanical component.

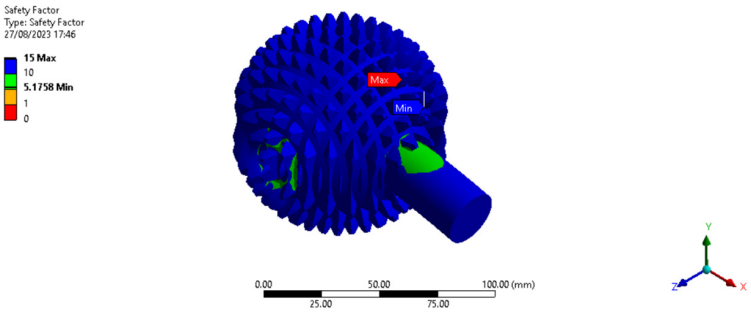

Fig. 12. Fatigue analysis: factor of safety

In Figure 13, the fatigue sensitivity of the crossed spherical gear is observed, evaluating an increase of 50% up to 600% of the established critical load; for that value of the increment, we have several cycles $1.39*10^5$ for the PEEK material, but evaluating an increase of 50% up to 3000% of the established critical load we obtained $4.27*10^5$ for Ti-6Al-4V material, and $5.39*10^5$ for AIS 304L material. This indicates that the cross-spherical gear life decreases, which agrees with the reference [61], so the minimum value recommended is 10^6 cycles. However, the increase limit for each material not to fail is 4.2 times the established load for PEEK material, 14 times for Ti-6Al-4V material, and 25 times for AISI 304L material.

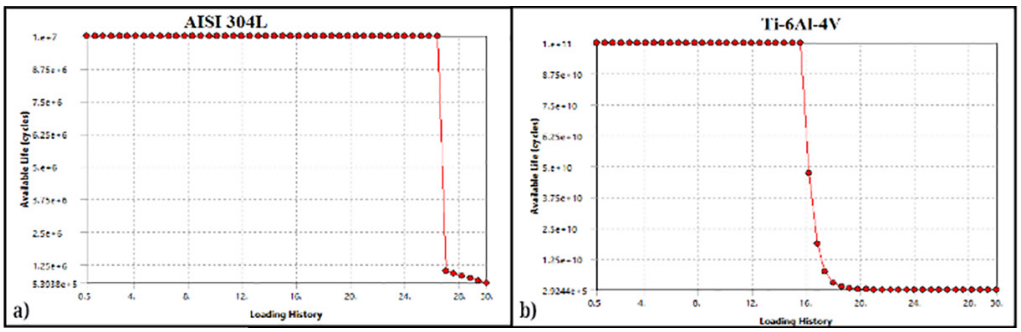

Fig. 13. *(Continued)*

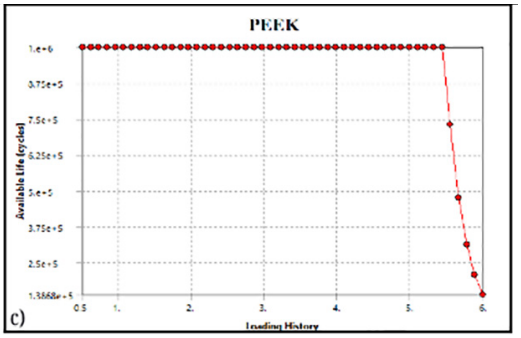

Fig. 13. Fatigue analysis. a) Fatigue sensitivity AISI 304L. b) Fatigue sensitivity Ti-6Al-4V. c) Fatigue sensitivity PEEK

4 CONCLUSIONS

In this study, simulation and finite element analysis of the cross-spherical gear, the central part of the ball joint with three degrees of freedom in a robotic prosthetic arm, was carried out using INVENTOR for modeling and ANSYS mechanical for numerical analysis. It was evaluated with three different materials to manufacture the cross-spherical gear considered under certain loading conditions like natural conditions; the results showed that the smallest value of total deformation and stresses occurred on the cross-spherical gear made of Ti-6Al-4V titanium alloy at the load value. This material has a higher safety factor than PEEK and AISI 304L due to the maximum performance, which is higher than titanium alloy. Similarly, with the high cycle fatigue analysis, the results indicate that they have good behavior and resistance to fluctuating and variable loads that produce fatigue failure. In addition, in the dynamic modal analysis, the natural frequencies and relevant vibration modes of the object of study were obtained, with vibration modes 1 and 3 having the highest mass participation. It was also observed that as the order of the vibration mode increased, so did the natural frequency. The stress concentration always occurs on the surface of the sphere and the base of the spherical gear tooth. Therefore, the maximum stress and strain values are acceptable to meet the design requirements, which gives us a good safety factor that the crossed spherical gear will work safely and correctly. In this way, the research objectives of the static, dynamic, and fatigue evaluation of the crossed spherical gear in a linear regime are fulfilled.

Finally, it should be noted that the gear modulus is inversely proportional to the number of gear teeth. This parameter is vital, as the number of teeth decreases as the modulus increases. Thus, the steps are greater, and the movements are sharper. Conversely, if the number of teeth decreases to obtain fine movements, the step is smaller, and the resistance of the gear tooth decreases. Consequently, a balance must be found between the prosthesis movements' resistance and fineness.

It is recommended that the effect of different lubricants, lubrication conditions, and wear on the crossed spherical gears be investigated to improve efficiency and prolong their service life. An operational modal analysis (OMA) must also be considered to determine the crossed spherical gear's dynamic behavior and operating frequencies.

5 REFERENCES

[1] A. I. Vásquez and J. U. Pérez, "Conceptual design of an alignment device for transfemoral prosthesis," *Rev. Fac. Ing.*, no. 102, pp. 108–114, 2022. https://doi.org/10.17533/udea.redin.20200805

[2] S. Bai, X. Li, and J. Angeles, "A review of spherical motion generation using either spherical parallel manipulators or spherical motors," *Mech. Mach. Theory*, vol. 140, pp. 377–388, 2019. https://doi.org/10.1016/j.mechmachtheory.2019.06.012

[3] S. Bai and J. Angeles, "The design of spherical multilobe-cam mechanisms," *Proc. Inst. Mech. Eng. Part C J. Mech. Eng. Sci.*, vol. 223, no. 2, pp. 473–482, 2009. https://doi.org/10.1243/09544062JMES1154

[4] N. M. Bajaj, A. J. Spiers, and A. M. Dollar, "State of the art in prosthetic wrists: Commercial and research devices," in *IEEE International Conference on Rehabilitation Robotics*, 2015, vol. 2015, pp. 331–338. https://doi.org/10.1109/ICORR.2015.7281221

[5] F. Patanè and P. Cappa, "A 3-DOF parallel robot with spherical motion for the rehabilitation and evaluation of balance performance," *IEEE Trans. Neural Syst. Rehabil. Eng.*, vol. 19, no. 2, pp. 157–166, 2011. https://doi.org/10.1109/TNSRE.2010.2089535

[6] S.-C. Yang, C.-K. Chen, and K.-Y. Li, "A geometric model of a spherical gear with a double degree of freedom," *J. Mater. Process. Technol.*, vol. 123, no. 2, pp. 219–224, 2002. https://doi.org/10.1016/S0924-0136(02)00067-5

[7] H.-C. Yang, "Using an imaginary planar rack cutter to create a spherical gear pair with continue involute teeth," *Arab. J. Sci. Eng.*, vol. 42, no. 11, pp. 4725–4735, 2017. https://doi.org/10.1007/s13369-017-2630-z

[8] S.-C. Yang, "A rack-cutter surface used to generate a spherical gear with discrete ring-involute teeth," *Int. J. Adv. Manuf. Technol.*, vol. 27, no. 1–2, pp. 14–20, 2005. https://doi.org/10.1007/s00170-004-2150-3

[9] L. Zhang, X. Lu, B. Wang, and X. Zhang, "Tooth surface modeling and stress analysis of 3-DOF spherical gear," in *Journal of Physics: Conference Series*, 2020, vol. 1570, no. 1. https://doi.org/10.1088/1742-6596/1570/1/012099

[10] K. Abe and R. Tadakuma, "Development of control method for active ball joint mechanism considering singularity of spherical gear," in *2021 IEEE/SICE International Symposium on System Integration (SII)*, 2021, pp. 690–695. https://doi.org/10.1109/IEEECONF49454.2021.9382684

[11] K. Abe, K. Tadakuma, and R. Tadakuma, "ABENICS: Active ball joint mechanism with three-DoF based on spherical gear meshings," *IEEE Trans. Robot.*, vol. 37, no. 5, pp. 1806–1825, 2021. https://doi.org/10.1109/TRO.2021.3070124

[12] T. Makino, S. Takaneka, Y. Sakai, H. Yoshikawa, and T. Kaito, "Impact of mechanical stability on the progress of bone ongrowth on the frame surfaces of a titanium-coated PEEK cage and a 3D porous titanium alloy cage: in vivo analysis using CT color mapping," *Eur. Spine J.*, vol. 30, no. 5, pp. 1303–1313, 2021. https://doi.org/10.1007/s00586-020-06673-4

[13] C. Gao *et al.*, "Enhancing antibacterial capability and osseointegration of polyetheretherketone (PEEK) implants by dual-functional surface modification," *Mater. Des.*, vol. 205, p. 109733, 2021. https://doi.org/10.1016/j.matdes.2021.109733

[14] O. K. Ajayi, B. O. Malomo, S. D. Paul, A. A. Adeleye, and S. A. Babalola, "Failure modeling for titanium alloy used in special purpose connecting rods," in *Materials Today: Proceedings*, 2021, vol. 45, pp. 4390–4397. https://doi.org/10.1016/j.matpr.2020.11.852

[15] J. Reginald, M. Kalayarasan, K. N. Chethan, and P. Dhanabal, "Static, dynamic, and fatigue life investigation of a hip prosthesis for walking gait using finite element analysis," *Int. J. Model. Simul.*, 2023. https://doi.org/10.1080/02286203.2023.2212346

[16] K. Moussaoui, M. Mousseigne, J. Senatore, R. Chieragatti, and P. Lamesle, "Influence of milling on the fatigue lifetime of a Ti6Al4V Titanium alloy," *Metals*, vol. 5, no. 3, pp. 1148–1162, 2015. https://doi.org/10.3390/met5031148

[17] A. T. Htoo, Y. Miyashita, Y. Otsuka, Y. Mutoh, and S. Sakurai, "Kinking behavior of S-N curve for Ti6Al4V alloy notched specimen under a load-controlled high cycle fatigue test," in *Metallurgy Technology and Materials IV*, 2016, vol. 867, pp. 39–44. https://doi.org/10.4028/www.scientific.net/MSF.867.39

[18] J. Lin, W. Li, S. Yang, and J. Zhang, "Vibration fatigue damage accumulation of Ti–6Al–4V under constant and sequenced variable loading conditions," *Metals*, vol. 8, no. 5, 2018. https://doi.org/10.3390/met8050296

[19] M. Belwanshi, P. Jayaswal, and A. Aherwar, "Mechanical behaviour investigation of PEEK coated titanium alloys for hip arthroplasty using finite element analysis," *Mater. Today Proc.*, vol. 56, pp. 2808–2817, 2022. https://doi.org/10.1016/j.matpr.2021.10.112

[20] J. Maximov, G. Duncheva, A. Anchev, V. Dunchev, and Y. Argirov, "Effect of diamond burnishing on fatigue behaviour of AISI 304 chromium-nickel austenitic stainless steel," *Materials (Basel).*, vol. 15, no. 14, 2022. https://doi.org/10.3390/ma15144768

[21] M. Wu, J. Mu, L. Zhuang, Y. Kong, and X. Zhou, "Fatigue analysis of injector body based on ANSYS workbench," in *Vibroengineering Procedia*, 2020, vol. 30, pp. 193–198. https://doi.org/10.21595/vp.2019.21183

[22] A. Heydari Astaraee, C. Colombo, and S. Bagherifard, "Insights on metallic particle bonding to thermoplastic polymeric substrates during cold spray," *Sci. Rep.*, vol. 12, no. 1, 2022. https://doi.org/10.1038/s41598-022-22200-5

[23] J. Zhang *et al.*, "Additively manufactured polyether ether ketone (PEEK) skull implant as an alternative to titanium mesh in cranioplasty," *Int. J. Bioprinting*, vol. 9, no. 1, pp. 173–180, 2023. https://doi.org/10.18063/ijb.v9i1.634

[24] Z. Ding, J. Ju, M. Ma, Y. Zhang, and J. Chen, "Tuberosity reconstruction baseplate for shoulder hemiarthroplasty: Morphological design and biomaterial application," *Front. Bioeng. Biotechnol.*, vol. 10, 2022. https://doi.org/10.3389/fbioe.2022.1047187

[25] M. Srivastava, A. Nag, L. Krejčí, J. Petrů, S. Chattopadhyaya, and S. Hloch, "Effect of periodic water clusters on AISI 304 welded surfaces," *Materials*, vol. 14, no. 1, 2021. https://doi.org/10.3390/ma14010210

[26] M. Srivastava, S. Hloch, L. Krejci, S. Chattopadhyaya, N. Gubeljak, and M. Milkovic, "Utilizing the water hammer effect to enhance the mechanical properties of AISI 304 welded joints," *Int. J. Adv. Manuf. Technol.*, vol. 119, no. 3, pp. 2317–2328, 2022. https://doi.org/10.1007/s00170-021-08357-9

[27] M. Srivastava, S. Hloch, L. Krejci, S. Chattopadhyaya, A. R. Dixit, and J. Foldyna, "Residual stress and surface properties of stainless steel welded joints induced by ultrasonic pulsed water jet peening," *Measurement*, vol. 127, pp. 453–462, 2018. https://doi.org/10.1016/j.measurement.2018.06.012

[28] G. Singh, R. K. Saxena, and S. Pandey, "An examination of mechanical properties of dissimilar AISI 304 stainless steel and copper weldment obtained using GTAW," in *Materials Today: Proceedings*, 2019, vol. 26, pp. 2783–2789. https://doi.org/10.1016/j.matpr.2020.02.579

[29] M. Duda, J. Pach, and G. Lesiuk, "Influence of polyurea composite coating on selected mechanical properties of AISI 304 steel," *Materials (Basel).*, vol. 12, no. 19, 2019. https://doi.org/10.3390/ma12193137

[30] L. Xie *et al.*, "Numerical analysis and experimental validation on residual stress distribution of titanium matrix composite after shot peening treatment," *Mech. Mater.*, vol. 99, pp. 2–8, 2016. https://doi.org/10.1016/j.mechmat.2016.05.005

[31] S. Kapoor *et al.*, "Evaluation of stress generated with different abutment materials and angulations under axial and oblique loading in the anterior maxilla: Three-dimensional finite element analysis," *Int. J. Dent.*, vol. 2021, 2021. https://doi.org/10.1155/2021/9205930

[32] A. Mestar, S. Zahaf, N. Zina, and A. Boutaous, "Numerical study of the effect of elastomer and cement of stress absorbers on the reduction of stresses in tibia and tibial bone analysed by finite element method," *Nano Biomed. Eng.*, vol. 10, no. 1, pp. 56–78, 2018. https://doi.org/10.5101/nbe.v10i1.p56-78

[33] A. K. Bhawe *et al.*, "Static structural analysis of the effect of change in femoral head sizes used in total hip arthroplasty using finite element method," *Cogent Eng.*, vol. 9, no. 1, 2022. https://doi.org/10.1080/23311916.2022.2027080

[34] M. G. Gok and O. Cihan, "Numerical analysis of the application of different lattice designs and materials for reciprocating engine connecting rods," *Sci. Iran.*, vol. 29, no. 5B, pp. 2362–2373, 2022. https://doi.org/10.24200/sci.2022.59400.6216

[35] X. Yang, C. Zhang, and L. Zhou, "Static analysis and optimization design of a special-shaped rod of the crab-like robot based on ANSYS Workbench," in *Journal of Physics: Conference Series*, 2023, vol. 2459, no. 1. https://doi.org/10.1088/1742-6596/2459/1/012136

[36] H. Song, L. Xu, X. Chen, W. Wei, and K. Liu, "Static and dynamic performance analysis of scissor seat of combine harvester," in *Journal of Physics: Conference Series*, 2021, vol. 2125, no. 1. https://doi.org/10.1088/1742-6596/2125/1/012042

[37] E. Osayande, K. P. Ayodele, and M. A. Komolafe, "Development of a robotic hand orthosis for stroke patient rehabilitation," *Int. J. Online Biomed. Eng.*, vol. 16, no. 13, pp. 142–149, 2020. https://doi.org/10.3991/ijoe.v16i13.13407

[38] W. Min, T. Qinglan, S. Chuanhong, and Y. Xiuyuan, "The design of robotic arm adaptive fuzzy controller based on oscillator and differentiator," *Int. J. Online Biomed. Eng.*, vol. 15, no. 5, pp. 47–68, 2019. https://doi.org/10.3991/ijoe.v15i05.8895

[39] G. Govindaraj and A. Selvakumar Arockia Doss, "Evaluation of robotic ankle-foot orthosis with different actuators using simscape multibody for foot-drop patients," *Int. J. Online Biomed. Eng.*, vol. 19, no. 10 SE-Papers, pp. 156–168, 2023. https://doi.org/10.3991/ijoe.v19i10.40375

[40] D. A. Najera-Flores and R. J. Kuether, "A study of whole joint model calibration using quasi-static modal analysis," *J. Vib. Acoust. Trans. ASME*, vol. 142, no. 5, 2020. https://doi.org/10.1115/1.4047247

[41] W. Yang and D. Jiang, "An improved rigid multibody model for the dynamic analysis of the planetary gearbox in a wind turbine," *Shock Vib.*, vol. 2016, 2016. https://doi.org/10.1155/2016/9742673

[42] Y. Su, L. Yao, and J. Zhang, "Contact dynamics analysis of nutation drive with double circular-arc spiral bevel gear based on mathematical modeling and numerical simulation," *Mech. Sci.*, vol. 12, no. 1, pp. 185–192, 2021. https://doi.org/10.5194/ms-12-185-2021

[43] Y. Cao, R. Zhong, D. Shao, Q. Wang, and X. Guan, "Dynamic analysis of rectangular plate stiffened by any number of beams with different lengths and orientations," *Shock Vib.*, vol. 2019, 2019. https://doi.org/10.1155/2019/2364515

[44] M. L. Puneeth and G. Mallesh, "Dynamic contact behavior of asymmetric spur gear," in *Materials Today: Proceedings*, 2021, vol. 44, pp. 2019–2027. https://doi.org/10.1016/j.matpr.2020.12.125

[45] W. Tanaś, J. Szczepaniak, J. Kromulski, M. Szymanek, J. Tanaś, and M. Sprawka, "Modal analysis and acoustic noise characterization of a grain crusher," *Ann. Agric. Environ. Med.*, vol. 25, no. 3, pp. 433–436, 2018. https://doi.org/10.26444/aaem/87154

[46] F. Concli, L. Cortese, R. Vidoni, F. Nalli, and G. Carabin, "A mixed FEM and lumped-parameter dynamic model for evaluating the modal properties of planetary gearboxes," *J. Mech. Sci. Technol.*, vol. 32, no. 7, pp. 3047–3056, 2018. https://doi.org/10.1007/s12206-018-0607-9

[47] B. Zheng, X. Wang, and J. Zhang, "Structure optimization design for brake drum based on response surface methodology," *Manuf. Technol.*, vol. 21, no. 3, pp. 413–420, 2021. https://doi.org/10.21062/mft.2021.045

[48] B. W. Lenggana *et al.*, "Effects of mechanical vibration on designed steel-based plate geometries: Behavioral estimation subjected to applied material classes using finite-element method," *Curved Layer. Struct.*, vol. 8, no. 1, pp. 225–240, 2021. https://doi.org/10.1515/cls-2021-0021

[49] L. O. B. Coronado *et al.*, "Finite element modal analysis and harmonic response analysis of a 3D printed vibration sensor enclosure," 2021. https://doi.org/10.1109/HNICEM54116.2021.9731919

[50] A. Vasu, J. Mei, J. Chung, and Y. Mehta, "Using weibull distribution function to determine the design bounds for carburized 4320 steel shafts subjected to bending dominated fatigue loading," *Int. J. Fatigue*, vol. 168, 2023. https://doi.org/10.1016/j.ijfatigue.2022.107447

[51] O. Bokůvka, M. Jambor, S. Hrček, J. Šteininger, F. Nový, and L. Trško, "Design of shaft respecting the fatigue limit for ultra-high number of cycles," *Period. Polytech. Transp. Eng.*, vol. 47, no. 1, pp. 6–12, 2019. https://doi.org/10.3311/PPtr.11562

[52] K. J. Nisbett and R. G. Budynas, *Shigley's Mechanical Engineering Design*. McGraw-Hill Education, 2014.

[53] J. Marin, *Mechanical Behavior of Engineering Materials*. Prentice-Hall, 1962.

[54] Z. Chen, B. Lei, L. Qin, G. Qiu, and A. Fuentes-Aznar, "Computerized design, simulation of meshing and stress analysis of external helical gear drives based on critical control points," *Energies*, vol. 15, no. 12, 2022. https://doi.org/10.3390/en15124290

[55] M. H. Vu, N. T. Huynh, K. N. Nguyen, A. S. Tran, and Q. M. Nguyen, "Optimal stress and strain of helical gear and rack in the steering system," *Math. Model. Eng. Probl.*, vol. 9, no. 3, pp. 697–706, 2022. https://doi.org/10.18280/mmep.090316

[56] Z. Qi *et al.*, "Contact stress reliability analysis based on first order second moment for variable hyperbolic circular arc gear," *Adv. Mech. Eng.*, vol. 14, no. 7, 2022. https://doi.org/10.1177/16878132221111210

[57] F. Mieth, C. Ulrich, and B. Schlecht, "Stress calculation on bevel gears with FEM influence vectors," *Forsch. im Ingenieurwesen/Engineering Res.*, vol. 86, no. 3, pp. 491–501, 2022. https://doi.org/10.1007/s10010-021-00550-2

[58] T. G. Yılmaz, G. Karadere, and F. Karpat, "A numerical analysis of hybrid spur gears with asymmetric teeth: Stress and dynamic behavior," *Machines*, vol. 10, no. 11, 2022. https://doi.org/10.3390/machines10111056

[59] H. He, H. Liu, C. Zhu, G. Li, and D. Chen, "Quantitative effect of residual stress on gear bending fatigue," *Jixie Gongcheng Xuebao/Journal Mech. Eng.*, vol. 59, no. 4, pp. 53–61, 2023. https://doi.org/10.3901/JME.2023.04.053

[60] F. Concli, L. Maccioni, L. Fraccaroli, and C. Cappellini, "Effect of gear design parameters on stress histories induced by different tooth bending fatigue tests: A numerical-statistical investigation," *Appl. Sci.*, vol. 12, no. 8, 2022. https://doi.org/10.3390/app12083950

[61] S. H. Budapanahalli, S. C. Dhaduti, and S. B. Mallur, "Fatigue analysis of hybrid aluminium 7075 composite gears," *J. Inst. Eng. Ser. D*, 2023. https://doi.org/10.1007/s40033-023-00499-2

6 AUTHORS

José L. Serna-Landivar is MSc Candidate in Mechanical Engineering from Pontificia Universidad Católica del Perú (PUCP) and Eng. in Mechanical Engineering from Universidad Tecnológica de Perú. Experience in computer-aided design in INVENTOR, SOLIDWORKS, STEEL ADVANCE, TEKLA STRUCTURES, and simulation with ANSYS SAP2000 computational tools. Research areas: Applied mechanics, mechanical design, finite element method for numerical solution of structural problems (E-mail: u18101283@utp.edu.pe).

Madelaine Violeta Risco Sernaqué, teacher in educational administration, research methodologist, professor at the Universidad Autónoma del Perú, completed a diploma and specializations in research methodology and research didactics (E-mail: mriscose@autónoma.edu.pe).

Ana Beatriz Rivas Moreano is Dr. in Public Management and Governance, teacher in educational administration, research methodologist, Professor at the Universidad Autónoma del Perú and the Universidad Tecnológica del Perú (UTP) (E-mail: arivasmor@autonoma.edu.pe).

William C. Algoner is a physics researcher, engineering educator, and scientific publication coordinator at the Universidad Tecnológica del Perú (UTP). Was a post-doctoral researcher at the Federal University of Parana, Brazil. He is currently an IEEE-UTP Student Branch Advisor (E-mail: walgoner@utp.edu.pe).

Daniela M. Anticona-Valderrama, Renacyt Researcher, Ph.D. in scientific research didactics, PhD in Public Management and Governance, Msc. in educational administration, graduate in physical mathematics, research teacher, engineering research methodology, 6 years' experience as a professor at the Universidad César Vallejo and the Universidad Tecnológica del Perú (UTP) (E-mail: daniela.anticona@upn.edu).

Walter Enrique Zúñiga Porras, Master in Educational Administration, Graduate from the Universidad Mayor de San Marcos, research methodologist, research coordinator of all careers at the Universidad Tecnológica del Perú (UTP) with more than 5 years of experience (E-mail: wzuniga@utp.edu.pe).

Carlos Oliva Guevara, Mechanical Engineer graduated from the UNI National Engineering University, Master's Degree in Education with a Mention in Education and University Teaching, Professional experience in Metal Mechanics and Hydraulic Power Plants, Academic Coordinator of the science area of the Universidad Tecnológica del Perú (UTP) headquarters (E-mail: coliva@utp.edu.pe).